Dalton Transactions

Oxidatively Stable Ferrocenyl-π-bridge-Titanocene D-π-A Complexes: An Electrochemical and Spectroscopic Investigation of the Mixed-Valence States

Journal:	*Dalton Transactions*
Manuscript ID	DT-ART-05-2018-001853.R1
Article Type:	Paper
Date Submitted by the Author:	06-Jul-2018

Complete List of Authors:	Pienkos, Jared; Furman University, Department of Chemistry Webster, Alex; Furman University, Department of Chemistry Piechota, Eric; University of North Carolina at Chapel Hill, Department of Chemistry Agakidou, Athina Danai; Furman University, Department of Chemistry McMillen, Colin; Clemson University, Department of Chemistry Pritchett, David; Furman University, Department of Chemistry Meyer, Gerald; University of North Carolina at Chapel Hill, Department of Chemistry Wagenknecht, Paul; Furman University, Department of Chemistry

Journal Name

ARTICLE

Oxidatively Stable Ferrocenyl-π-bridge-Titanocene D-π-A Complexes: An Electrochemical and Spectroscopic Investigation of the Mixed-Valence States

Received 00th January 20xx,
Accepted 00th January 20xx

DOI: 10.1039/x0xx00000x

www.rsc.org/

Jared A. Pienkos,[a] Alex B. Webster,[a] Eric J. Piechota,[b] A. Danai Agakidou,[a] Colin D. McMillen,[c] David Y. Pritchett,[a] Gerald J. Meyer,[b] and Paul S. Wagenknecht.*[a]

The synthesis, spectroscopic, and electrochemical characterization of oxidatively stable D-π-A compounds of the form $(Me_2CpC_2Fc)_2TiCl_2$ and $^{R}Cp_2Ti(C_2Fc)_2CuX$ (where Fc = ferrocenyl) are reported. Oxidative stability enabled by the addition of CuX is evidenced by voltammagrams of the $^{R}Cp_2Ti(C_2Fc)_2CuX$ compounds which all display two chemically-reversible $1e^-$ $Fe^{III/II}$ couples, indicative of electronic communication between the Fc- termini. Differential pulse voltammetry (DPV) in CH_2Cl_2 / [*n*-Bu_4N][PF_6], demonstrated that the redox potential differences between the two $1e^-$ $Fe^{III/II}$ couples ($\Delta E_{1/2}$) is between 112 mV and 146 mV, being most pronounced with the electron rich $Cp^*_2Ti(C_2Fc)_2CuBr$. The $\Delta E_{1/2}$ values were unaffected by solvent (THF) and displayed only a small dependence on the identity of the counterion, either PF_6^- or $B(C_6F_5)_4^-$. For each complex with a measurable $\Delta E_{1/2}$ value, spectroelectrochemical experiments were performed in CH_2Cl_2 / [*n*-Bu_4N][PF_6] and gave clear evidence of both the one-electron oxidized mixed-valent (MV) state and the two-electron oxidized state, each with distinct spectroscopic signatures. The MV states of these complexes showed absorbance between 820 and 940 nm which were replaced with a higher energy feature following a second oxidation. A very similar absorption band was also observed in the one-electron oxidized state of an analogue with only a single Fc substituent, namely $^{TMS}Cp_2Ti(C_2Fc)(C_2Ph)CuBr$, suggesting this feature is not an Fe^{II}/Fe^{III} intravalence charge-transfer (IVCT) band. Despite DFT calculations suggesting a pathway exists for electronic coupling, NIR spectroscopy on the MV states gave no evidence of an Fe^{II}/Fe^{III} IVCT. Possible contributions to $\Delta E_{1/2}$ from inductive effects and a superexchange mechanism are discussed.

Introduction

Compounds that have electron donors (D) attached through π-bridges to electron acceptors (A), termed D-π-A compounds, have many promising applications including non-linear optical (NLO) materials,[1] photovoltaics,[2, 3] and probing electronic communication through molecular wires.[4] Ferrocene, because of its electron donating properties, ease of functionalization, and well behaved electrochemistry, has been incorporated as the donor in D-π-A compounds.[5-14] Such ferrocenyl (Fc-) compounds also have been investigated for NLO properties (e.g., Fig. 1, **a**)[6, 7] and as dyes for dye-sensitized solar cells (DSSCs, e.g., Fig. 1, **b**).[8-13]

Recently, we have investigated D-π-A constructs containing Fc-donors and titanocene acceptors (e.g., Fig. 1, **c**) that have properties, which make them suitable for the aforementioned applications.[14] For instance, $Cp_2Ti(C_2Fc)_2$ (where C_2Fc = ethynylferrocene) has a low energy (LE) absorbance band ascribed to an Fe^{II} to Ti^{IV} metal-to-metal charge transfer (MMCT). This LE band exhibits solvatochromism, suggesting that the titanocene may display NLO properties.[15, 16] Moreover, the excited state $Cp_2Ti(C_2Fc)_2^{+/0}$ potential was estimated to be more negative than -1.55 V vs $FcH^{+/0}$. This suggests that $Cp_2Ti(C_2Fc)_2$, and similarly structured D-π-A constructs with titanocene acceptors, may be potent excited state reducing agents, useful as dyes in DSSCs. However, these compounds decompose upon oxidation, which would hamper their use as excited state reductants. In this report we discuss two strategies to enhance oxidative stability: 1) appending the donor group to the Cp ligand (i.e, $(Me_2CpC_2Fc)_2TiCl_2$, Fig. 2)[17, 18] thus avoiding weaker titanium alkynyl bonds that cleave upon oxidation (*vida infra*) or 2) complexing a copper halide in between the alkynes, which was previously utilized by Lang et al. to generate the oxidatively stable $^{TMS}Cp_2Ti(C_2Fc)_2CuBr$ species (Fig. 2).[19]

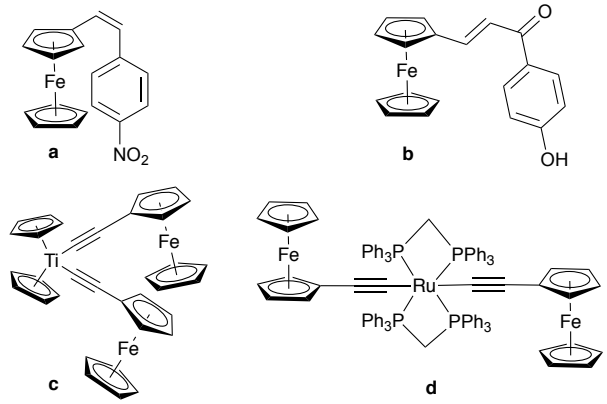

Fig. 1: Ferrocenyl compounds discussed herein, which were investigated as NLO materials (**a**), dyes for DSSCs (**b**, **c**), and utilized to probe electronic communication through a π-M-π bridge (**d**).

[a] *Department of Chemistry, Furman University, Greenville, SC, 29613, USA.*
[b] *Department of Chemistry, The University of North Carolina at Chapel Hill, Chapel Hill, NC, 27599, USA.*
[c] *Department of Chemistry, Clemson University, Clemson, SC, 29634, USA.*
†Electronic Supplementary Information (ESI) available: CCDC 1852310 and 1852311. For ESI and crystallographic data in CIF see DOI: 10.1039/x0xx00000x

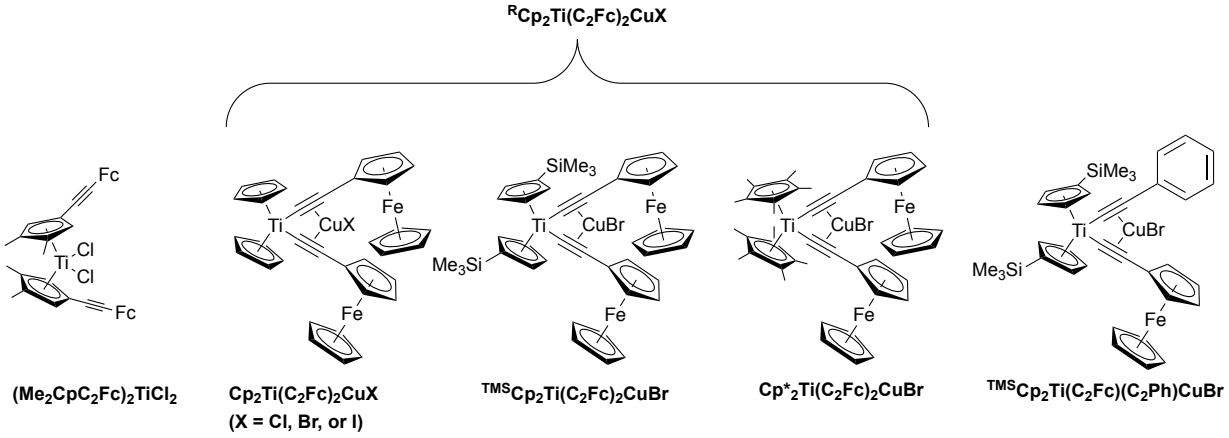

Fig. 2: Target compounds and abbreviations for these species.

Additionally, systems with Fc- groups linked through a π-bridge to a central metal (M) have been utilized to probe electronic communication. Pioneering work by Wolf et al. showed the interaction between the two Fc- groups in *trans*-$[Ru(dppm)_2(C_2Fc)_2]$ (Fig 1., d) is greater than the analogous interaction in FcC_4Fc.[20] This is demonstrated by the larger $\Delta E_{1/2}$ value ($\Delta E_{1/2} = E_{1/2}^2 - E_{1/2}^1$) of the two inequivalent $Fe^{III/II}$ redox couples in the ruthenium system as compared to FcC_4Fc. The value of $\Delta E_{1/2}$ indicates the stability of the mixed-valent (MV) state (A^+) relative to its disproportionation products (eq 1).

$$A^{2+} + A \rightleftharpoons 2\,A^{+} \quad K_c = e^{\frac{nF\Delta E_{1/2}}{RT}} \qquad (1)$$

Though $\Delta E_{1/2}$ values often correlate with electronic coupling, spectroscopic studies of the MV states are necessary to evaluate the extent of such coupling as there are many cases where such correlations are not evident.[21] Indeed, electronic coupling between the terminal Fc in the $1e^-$ oxidized species, *trans*-$[Ru(dppm)_2(C_2Fc)_2]^+$ is evidenced from analysis of the IVCT transitions in the NIR which suggested stepwise coupling through a non-innocent redox-active bridge.[22] It has also been shown that the nature of the metal in the π-M-π system can influence the stability of the MV species, Fc^+-π-M-π-Fc. This can be observed in the comparison of *trans*-$[Pt(PPh_3)_2(C_2Fc)_2]$, *trans*-$[Ru(dppm)_2(C_2Fc)_2]$, and *trans*-$[Cr(cyclam)(C_2Fc)_2]$, which show $\Delta E_{1/2}$ values of 260 mV, 220 mV, and 65 mV, respectively.[20, 23, 24]

Because of interest in electronic transport in π-M-π systems, other M bridging systems have been recently investigated. A common architecture for such species utilizes C_2Fc ligands directly bound to an organometallic fragment. However, when C_2Fc is appended to a titanocene framework, e.g., $^{TMS}Cp_2Ti(C_2Fc)_2$, cyclic voltammetry shows no evidence of electronic communication.[25] Nevertheless, while studying the oxidative stability of D-π-A constructs with titanocene acceptors, we discovered that electronic communication between the two Fc- groups is observed upon insertion of Cu^I into $Cp_2Ti(C_2Fc)_2$. Specifically, well separated $Fe^{III/II}$ couples were observed for each Fc unit when Cu^I was present, while only a single irreversible oxidation was observed in the absence of copper. The significant $\Delta E_{1/2}$ observed in the presence of Cu^I is indicative of electronic communication between the two Fc units. Because electrochemical evidence does not represent unambiguous proof of electronic coupling,[21] we report complementary analyses, including spectroscopic data on the one electron oxidized MV state and the two-electron oxidized form, each with distinct spectroscopic signatures.

Results and Discussion

Synthesis and Characterization of Oxidatively Stable Species

Attachment of the Fc- donor to the Cp ring was achieved by 1,2-nucleophilic addition of LiC_2Fc to 3,4-dimethylcyclopent-2-en-1-one followed by dehydration with HCl.[18] The resulting substituted cyclopentadienyl ring was then deprotonated with *n*-BuLi and treated with $TiCl_4$ in order to generate a titanocene with the donor appended to the Cp ring (Scheme 1).

Following a modification of the literature methods for the synthesis of $^{TMS}Cp_2Ti(C_2Fc)_2CuBr$,[19] $Cp_2Ti(C_2Fc)_2CuBr$ was prepared by treatment of $Cp_2Ti(C_2Fc)_2$ with CuBr in THF (Scheme 2). The product was isolated by concentrating the reaction solution, purifying the resulting solid using column chromatography (5 % TEA in CH_2Cl_2), and reprecipitating the solid from a CH_2Cl_2/hexanes mixture, giving $Cp_2Ti(C_2Fc)_2CuBr$. For comparison, $^{TMS}Cp_2Ti(C_2Fc)_2CuBr$,[19] $Cp_2Ti(C_2Fc)_2CuCl$, $Cp_2Ti(C_2Fc)_2CuI$, $Cp^*_2Ti(C_2Fc)_2CuBr$, and $Cp_2Ti(C_2Ph)_2CuBr$ were synthesized in an analogous fashion. The structures of $Cp_2Ti(C_2Fc)_2CuBr$ and $Cp^*_2Ti(C_2Fc)_2CuBr$ were confirmed using X-ray crystallography (Fig. 3).

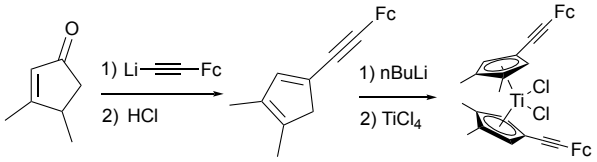

Scheme 1: Synthesis of $(Me_2CpC_2Fc)_2TiCl_2$

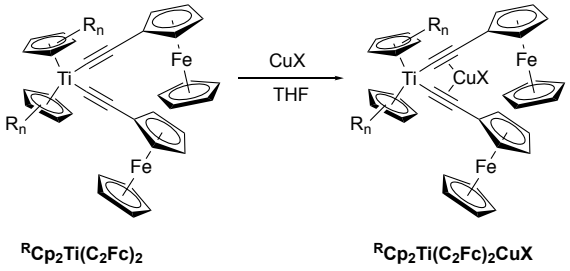

Scheme 2: Coordination of copper halides (CuX) in between the alkynes of $^RCp_2Ti(C_2Fc)_2$ to form $^RCp_2Ti(C_2Fc)_2CuX$.

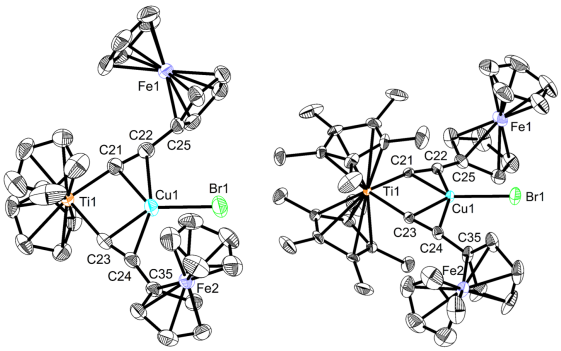

Fig. 3: Structures of $Cp_2Ti(C_2Fc)_2CuBr$ (left) and $Cp^*_2Ti(C_2Fc)_2CuBr$ (right). H-atoms omitted for clarity. Key bond lengths and angles for $Cp_2Ti(C_2Fc)_2CuBr$ and $Cp^*_2Ti(C_2Fc)_2CuBr$, respectively: Cu(1)-C(21), 2.073(3), 2.046(2); Cu(1)-Cu(22), 2.300(3), 2.141(2); Cu(1)-Cu(23), 2.059(3), 2.088(2); Cu(1)-Cu(24), 2.192(3), 2.219(3); Cu(1)-Ti(1), 2.8901(6), 2.9310(6); C(21)-C(22), 1.222(4), 1.235(4); C(23)-C(24), 1.233(4), 1.231(4); C(21)-Ti(1)-C(23), 91.13(10), 89.60(9).

An analogue with a single ethynylferrocene ligand, $^{TMS}Cp_2Ti(C_2Fc)(C_2Ph)CuBr$ was also synthesized according to the aforementioned strategy. However, due to higher solubility, no reprecipitating strategy was employed after column chromatography, and a simple hexanes wash was sufficient for purification. All compounds are air stable in solution and in the solid state and were characterized by elemental analysis, ^{1}H- and ^{13}C-NMR spectroscopy, UV-Visible spectroscopy, IR-spectroscopy, cyclic voltammetry (CV), and differential pulse voltammetry (DPV).

The ^{1}H-NMR spectra of all bimetallic compounds have two doublets of doublets ($J_1 = J_2 =$ ~1.78 Hz), which appear as triplets, representing the protons on the substituted Fc- ring, and a singlet between 4.0-5.0 ppm for the protons on the unsubstituted Fc- ring. In the $Cp_2Ti(C_2Fc)_2CuX$ species, a singlet between 6.0-6.5 ppm is representative of the protons on the Cp ring bound to titanium. Although ^{1}H-NMR resonances slightly shift upon complexation of Cu^I, vibrational spectroscopy is more diagnostic of this insertion. For instance, upon coordination of Cu^I into $Cp_2Ti(C_2Fc)_2$ to generate $Cp_2Ti(C_2Fc)_2CuBr$, a shift of $\upsilon_{C\equiv C}$ from 2053 cm^{-1} to 2006 cm^{-1} occurs, in agreement with previous examples where Cu^I was coordinated between the alkynes.[19, 26, 27]

The voltammogram of $Cp_2Ti(C_2Fc)_2$ without coordinated Cu^I shows a single chemically irreversible 2e$^-$ $Fe^{III/II}$ couple in the anodic scan followed by a chemically reversible 2e$^-$ wave (Fig. 4). The fact that the first 2e$^-$ $Fe^{III/II}$ couple is unsplit has been ascribed to the lack of electronic communication via the C_2TiC_2 linkage.[14, 25, 28] The irreversible nature of this oxidation has been attributed to subsequent rapid heterolytic Ti–C bond cleavage. During this cleavage, 1e$^-$ from each Ti–C bond serves to reduce Fc^+ back to Fc, while the remaining e$^-$ is involved in the formation of a new C–C bond to generate FcC_4Fc (eq 2).

$$Cp_2Ti(C_2Fc)_2 \xrightarrow{-2e^-} Cp_2Ti(C_2Fc^+)_2 \longrightarrow [Cp_2Ti^{IV}]^{2+} + FcC_4Fc \quad \textbf{(2)}$$

The reversible oxidation of FcC_4Fc appears slightly anodic of the first irreversible oxidation and consists of two closely spaced 1e$^-$ $Fe^{III/II}$ couples (Fig. 4).[14, 25] These same features occur for $^{TMS}Cp_2Ti(C_2Fc)_2$[25] and $Cp^*_2Ti(C_2Fc)_2$ (Supporting Information).[14] The heterosubstituted monoferrocenyl complex, $^{TMS}Cp_2Ti(C_2Fc)(C_2Ph)$ also undergoes oxidative degradation, giving FcC_4Ph as the major product.[14]

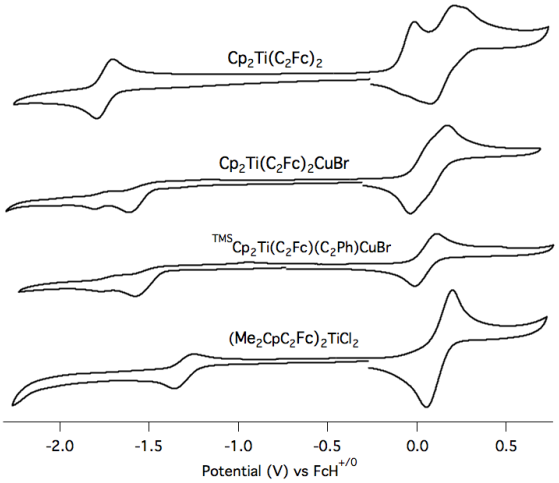

Fig. 4: Cyclic voltammograms of $Cp_2Ti(C_2Fc)_2$, $Cp_2Ti(C_2Fc)_2CuBr$, $^{TMS}Cp_2Ti(C_2Fc)(C_2Ph)CuBr$, and $(Me_2CpC_2Fc)_2TiCl_2$. Conditions: [Ti] ~ 1 mM in CH_2Cl_2 (0.1 M [*n*-Bu_4N][ClO_4]), glassy carbon working electrode, Ag^+/Ag reference electrode, and scan rate = 100 mV/s. The x-axis reports voltage vs FcH as determined by recording a voltammogram of FcH before and after data collection. Voltage sweeps are initiated in the cathodic direction.

The oxidative decomposition is prevented when CuBr is coordinated between the alkynes as demonstrated by the chemical reversibility of the $Fe^{III/II}$ redox couple (Fig. 4) for $Cp_2Ti(C_2Fc)_2CuBr$ (2e$^-$) and $^{TMS}Cp_2Ti(C_2Fc)(C_2Ph)CuBr$ (1e$^-$). The voltammograms for $^{TMS}Cp_2Ti(C_2Fc)_2CuBr$ and $Cp^*_2Ti(C_2Fc)_2CuBr$ also show chemically reversible $Fe^{III/II}$ couples (*vide infra*). It is likely that Cu^I prevents the geometric rearrangements necessary for heterolytic cleavage and diyne formation.

The other method used to prevent oxidative degradation involved attaching the donor directly to the Cp ring, avoiding the oxidatively labile Ti–C bond. The cyclic voltammogram of $(Me_2CpC_2Fc)_2TiCl_2$ shows a chemically reversible 2e$^-$ $Fe^{III/II}$ couple (Fig. 4) based on comparison of the peak current to other Fc- titanocene compounds at known concentrations. This demonstrates that linking the donor to the titanocene through a C–C bond rather than a weaker Ti–C bond indeed stabilizes the complex to oxidation.

Electronic Communication

While the oxidative stability of $(Me_2CpC_2Fc)_2TiCl_2$ and the $^RCp_2Ti(C_2Fc)_2CuBr$ complexes may be beneficial for applications involving excited state e$^-$ transfer, the most notable feature in the electrochemistry for these compounds is that upon insertion of Cu^I, two separate $Fe^{III/II}$ couples are observed. As shown in Fig. 5, $Cp_2Ti(C_2Fc)_2CuBr$, $^{TMS}Cp_2Ti(C_2Fc)_2CuBr$, and $Cp^*_2Ti(C_2Fc)_2CuBr$ display redox couples in the anodic scan in CH_2Cl_2/[*n*-Bu_4N][PF_6] that are split, suggesting two closely spaced one-electron couples. The absence of an anodic feature in the analogous voltammogram for $Cp_2Ti(C_2Ph_2)_2CuBr$ (Fig. 5) precludes ascribing either feature in the $^RCp_2Ti(C_2Fc)_2CuX$ complexes to a $Cu^{II/I}$ redox couple.

The $\Delta E_{1/2}$ values for the inequivalent $Fe^{III/II}$ couples were measured from the peak-to-peak separation in the DPV (Fig. 6), as determined by Gaussian fitting (Supporting Information), giving $\Delta E_{1/2}$ values of 112 mV, 122 mV, and 146 mV for $Cp_2Ti(C_2Fc)_2CuBr$, $^{TMS}Cp_2Ti(C_2Fc)_2CuBr$, and $Cp^*_2Ti(C_2Fc)_2CuBr$, respectively. These

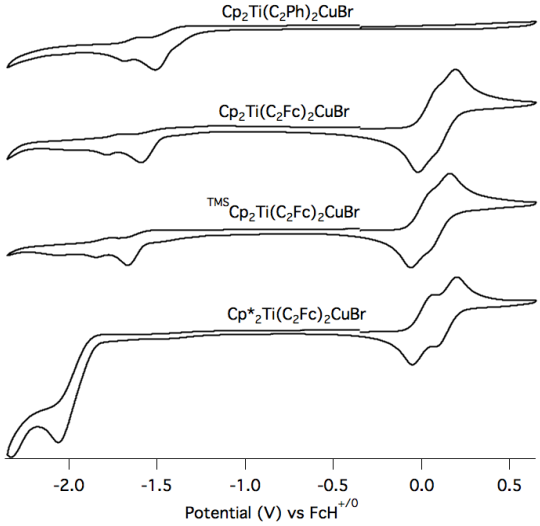

Fig. 5: Conditions indicated in Fig. 3 except the supporting electrolyte is [*n*-Bu_4N][PF_6]. Voltage sweeps are initiated in the anodic direction.

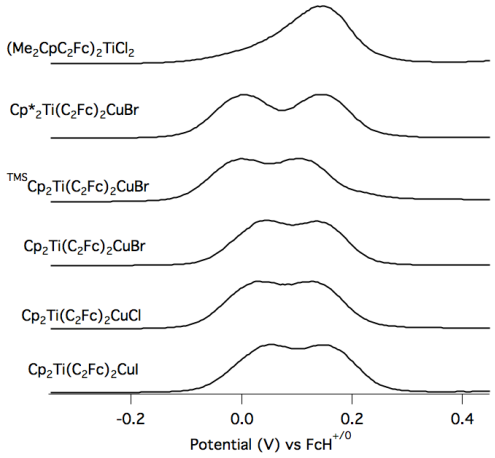

Fig 6: DPVs of complexes discussed herein. Conditions indicated in Fig 4. Parameters: step E = 4 mV, pulse width = 50 ms, pulse period = 200 ms, and pulse amplitude = 10 mV.

$\Delta E_{1/2}$ values are in agreement with those obtained from spectroelectrochemical experiments (Table 1). This splitting was not previously observed in a report that discussed the electrochemistry of $^{TMS}Cp_2Ti(C_2Fc)_2CuBr$ in THF.[19] This oversight is likely due to broadening of electrochemical features in THF due to higher uncompensated resistance, which is not as significant in CH_2Cl_2.[29,30] Indeed, performing these electrochemical experiments in THF under the same conditions showed that the spacing between the two $Fe^{III/II}$ couples is less apparent. However, the $\Delta E_{1/2}$ values calculated by Gaussian deconvolution of the DPVs produced $\Delta E_{1/2}$ values within 5% of those observed in CH_2Cl_2 (Supporting information, Table 1).

Although the splitting in the CVs and DPVs suggests that the Fc-termini in $^{R}Cp_2Ti(C_2Fc)_2CuX$ are in electronic communication, such communication is not apparent for $(Me_2CpC_2Fc)_2TiCl_2$. However, the DPV for $(Me_2CpC_2Fc)_2TiCl_2$ is broad, which may suggest two closely spaced $1e^-$ $Fe^{III/II}$ waves. A method developed by Taube and Richardson[31] allows the determination of $\Delta E_{1/2}$ values from DPV peak widths at half height, which is particularly useful in cases where two redox events are unresolved. There are specific parameters that need to be used for this experiment and these were indeed used for the data in Fig. 6. Using this method, the peak width for $(Me_2CpC_2Fc)TiCl_2$ of 148 mV gives a $\Delta E_{1/2}$ value of 74 mV. Such a method has frequently been used to determine $\Delta E_{1/2}$ values in non-aqueous solvents.[24, 32-39] However, the paper describing this method gives a cautionary note, suggesting that it should only be used for electrode processes approaching theoretical reversible behavior.[31]

Using the titanocene systems discussed herein, we have an opportunity to investigate whether $\Delta E_{1/2}$ values calculated using DPV peak widths in non-aqueous solvent systems accurately reflect the observed $\Delta E_{1/2}$ values measured as the peak-to-peak separation in the DPV. The data in Table 2 shows that the $\Delta E_{1/2}$ values calculated from peak width overestimate the $\Delta E_{1/2}$ values determined from peak-to-peak separation under these conditions. For instance, $Cp_2Ti(C_2Fc)_2CuBr$ has an observed $\Delta E_{1/2}$ value of 112 mV, whereas that calculated from the peak width is 129 mV. This overestimation underscores the assertion that $\Delta E_{1/2}$ values calculated solely from DPV peak widths should be viewed with some caution if theoretical reversible behavior is not also demonstrated.[31] Certainly there are cases where such concerns can be mitigated with additional experimental evidence,[39] but in heeding this cautionary note, we cannot definitively assign a value of $\Delta E_{1/2}$ to $(Me_2CpC_2Fc)_2TiCl_2$.

Table 1. Comparison of electrochemical and spectroelectrochemical data.

	[*n*-Bu_4N][PF_6]/CH_2Cl_2 Electrochemistry (Spectroelectrochemistry)				[*n*-Bu_4N][PF_6]/THF	[*n*-Bu_4N][$B(C_6F_5)_4$]/CH_2Cl_2
Compound	$E_{1/2}(1)$ (V)[a, b]	$E_{1/2}(2)$ (V)[a, b]	$\Delta E_{1/2}$ (mV)	K_c	$\Delta E_{1/2}$ (mV)	$\Delta E_{1/2}$ (mV)
$Cp^*_2Ti(C_2Fc)_2CuBr$	0.001 (0.007)	0.147 (0.146)	146 (139)	293 (225)	140	163
$^{TMS}Cp_2Ti(C_2Fc)_2CuBr$	0.017 (0.052)	0.139 (0.171)	122 (119)	115 (103)	116	147
$Cp_2Ti(C_2Fc)_2CuBr$	0.034 (0.042)	0.146 (0.152)	112 (110)	78 (73)	112	144
$Cp_2Ti(C_2Fc)CuCl$	0.022 (0.051)	0.138 (0.162)	116 (111)	91 (75)	-	-
$Cp_2Ti(C_2Fc)CuI$	0.029 (–)	0.141 (–)	112 (–)	78 (–)	-	-
$^{TMS}Cp_2Ti(C_2Fc)(C_2Ph)CuBr$	0.051[c] (0.090)	-	-		-	-
$(Me_2CpC_2Fc)_2TiCl_2$	0.128[c] (0.168)	-	-		-	-

[a] All electrochemical $E_{1/2}$ values are from Gaussian fits of the DPV unless otherwise noted. [b] All potentials are reported vs $FcH^{+/0}$ [c] From the cyclic voltammogram.

Table 2. Comparison of calculated and observed $\Delta E_{1/2}$ values data.

Compound	PWHH[a]	Calculated $\Delta E_{1/2}$[b]	Observed $\Delta E_{1/2}$[c]
$(Me_2CpC_2Fc)_2TiCl_2$	148	74	N/A
$Cp^*_2Ti(C_2Fc)_2CuBr$	264	180	146
$^{TMS}Cp_2Ti(C_2Fc)_2CuBr$	236	146	122
$Cp_2Ti(C_2Fc)_2CuBr$	218	129	112

[a]The peak width at half height (PWHH) is measured in mV. [b]$\Delta E_{1/2}$ values (mV) were calculated from PWHH values using Table 1 in reference 31. [c]The $\Delta E_{1/2}$ values (mV) were determined from the Gaussian fit of peak-to-peak separation in the DPV.

Communication Through Space vs Communication Through-Bond

The choice of supporting electrolyte can significantly alter the extent of interaction between redox active termini.[21, 40] For example, the $\Delta E_{1/2}$ value associated with the stepwise oxidation of bis(fulvene)dinickel (Fig. 7, **a**) decreases from 744 mV to 480 mV by changing the supporting electrolyte from $[n\text{-}Bu_4N][B(C_6F_5)_4]$ to $[n\text{-}Bu_4N][PF_6]$.[41] For *ortho*-bis(ferrocenylethynyl)benzene (Fig. 7, **b**) two 1 e^- $Fe^{III/II}$ couples were observed ($\Delta E_{1/2}$ = 150 mV) in CH_2Cl_2 when $[n\text{-}Bu_4N][B(C_6F_5)_4]$ was used as the supporting electrolyte, whereas when using $[n\text{-}Bu_4N][PF_6]$, a single 2 e^- $Fe^{III/II}$ couple was observed.[42] In both cases, the authors attributed the decrease in $\Delta E_{1/2}$ to decreased electrostatic (through space) interactions that occur when ion-pairing between the supporting electrolyte and the oxidized species is increased (i.e., ion pairing with PF_6^- is stronger than ion pairing with $B(C_6F_5)_4^-$).[41, 42]

A key question for the compounds investigated herein is whether the observed redox splitting is dominated by through-space or through-bond interactions. While no through-space electronic communication is observed for *ortho*-bis(ferrocenylethynyl)benzene (Fig. 7, **b**) in the $[n\text{-}Bu_4N][PF_6]/CH_2Cl_2$ solvent/electrolyte system, the similarly structured $^RCp_2Ti(C_2Fc)_2CuX$ derivatives display $\Delta E_{1/2}$ values between 112 mV and 146 mV in the same solvent/electrolyte system. Data from the crystal structures show that for 4,5-bis(ferrocenylethynyl)phthalonitrile (Fig. 7, **c**) the distance between the bound Fc- carbons (d_{cc}, Fig. 7) is 5.52 Å,[43] which is closer than the analogous distance in $Cp_2Ti(C_2Fc)_2CuBr$ (6.60 Å, Fig. 3), $Cp^*_2Ti(C_2Fc)_2CuBr$ (6.28 Å, Fig. 3) and $^{TMS}Cp_2Ti(C_2Fc)_2CuBr$ (6.10 Å).[19] Since electrostatic interactions are less pronounced over longer distances, it is likely that the $\Delta E_{1/2}$ values in the $^RCp_2Ti(C_2Fc)_2CuX$ derivatives are not due to through-space, electrostatic interactions. Our choice of comparing the distances between the bound Fc-carbons is out of recognition that the distance between the Fe centers is dependent on the conformation of the two Fc substituents, which likely rotate around the alkynyl-Fc single bond in solution. Because the averaged Fe-Fe distances in solution may not be accurately reflected by any solid-state structural measurement, these distance arguments should be viewed with at least some caution.

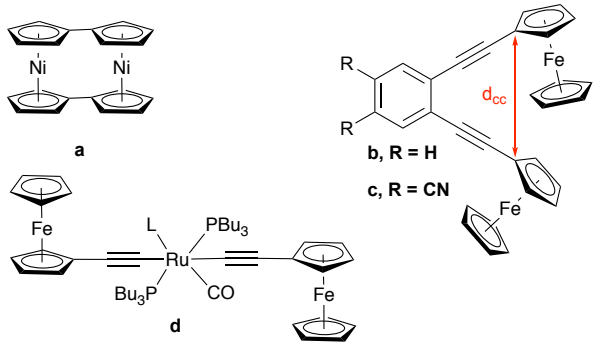

Fig 7: Bis(fulvene)dinickel (**a**), *ortho*-bis(ferrocenylethynyl)benzene (**b**), 4,5-bis(ferrocenylethynyl)phthalonitrile (**c**), and *trans*-(Fc-C≡C)$_2$(PBu$_3$)$_2$Ru(CO)(L) (**d**). Compounds previously investigated for electronic communication

Similar distance arguments have been used to describe electronic communication through a thiophene bridge. Iyoda et al. showed that the $\Delta E_{1/2}$ for 2,5-diferrocenylthiophene is larger than the $\Delta E_{1/2}$ for 3,4-diferrocenylthiophene despite a larger distance between the redox active termini, thus a through-bond interaction was inferred.[44, 45] This was confirmed by UV-vis/near-IR spectroelectrochemical studies, which showed that the Fc- termini are more strongly coupled in the 2,5-diferrocenylthiophene than in 3,4-diferrocenylthiophene.[46]

To determine if through-space, electrostatic communication can be increased for the complexes investigated herein, CVs and DPVs were recorded using a supporting electrolyte with a weakly coordinating anion, namely $B(C_6F_5)_4^-$ (Supporting Information). The $\Delta E_{1/2}$ values for $Cp_2Ti(C_2Fc)_2CuBr$, $^{TMS}Cp_2Ti(C_2Fc)_2CuBr$, and $Cp^*_2Ti(C_2Fc)_2CuBr$ increased by only 16-32 mV (Table 1), which is small compared to the change observed for *ortho*-bis(ferrocenylethynyl)benzene (*vide supra*). Again, this may reflect the fact that in solution the Fc- groups in the $^RCp_2Ti(C_2Fc)_2CuBr$ compounds are farther apart than the Fc- groups in *ortho*-bis(ferrocenylethynyl)benzene, and that even with a weakly coordinating anion, electrostatic communication is quite small. This suggests that the majority of the electronic communication is indeed through-bond. However, a demonstration that through-bond communication likely contributes to the redox splitting does not necessarily imply electronic coupling. Inductive effects are also possible.[21] To investigate possible mechanisms for such communication, DFT studies and spectroscopic studies on the MV states were performed.

Computational and Spectroscopic Investigations

DFT calculations were performed on $Cp_2Ti(C_2Fc)_2CuBr$, employing the ωB97XD/def2-TZV functional and basis. The solvent medium is represented by the Tomasi polarizability continuum assigned the macroscopic dielectric constant of CH_2Cl_2. The HOMO of $Cp_2Ti(C_2Fc)_2CuBr$ (Figure 8) indicates that the bridging CuBr contributes significant electron density to this orbital, suggesting that electronic coupling through the Cu^I bridge is possible.

Given this possible pathway for electronic coupling and the relatively large K_c values for several of the complexes investigated herein, spectroelectrochemical measurements (400-1100 nm) and redox titrations (850 – 2200 nm) were performed in order to analyze the spectroscopic properties of the MV state. For all complexes with measurable $\Delta E_{1/2}$ values, the application of potentials positive of the $Fe^{III/II}$ redox couple resulted in spectral changes indicative of two consecutive, one-electron oxidation events. This is further supported by the observation of two sets of isosbestic points (Figure 9 and

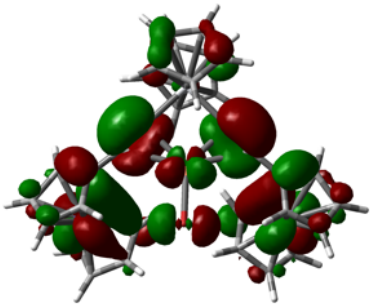

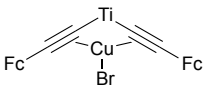

Fig 8: HOMO of $Cp_2Ti(C_2Fc)_2CuBr$.

Supporting Information). The compounds were found to have chemically reversible oxidations on the time scale of the experiment by also recording spectra during a reverse step-wise scan. In a typical case, 90% of the initial absorbance was recovered (Supporting Information). Single wavelength data were fit to two a sum of two Nernst equations for the consecutive oxidation events, giving $E_{1/2}$ and $\Delta E_{1/2}$ values in good agreement with those determined from DPV (Table 1). Using previously described methods,[47] the spectrum of the 1e⁻ oxidized MV state was corrected for comproportionation and reconstructed. In brief, this is accomplished by using the experimental spectrum of the neutral ground state, the spectroelectrochemically determined spectrum of the 2e⁻ oxidized state, and a spectrum with suitable concentrations of all three species and the corresponding fractional concentration. The spectrum at the applied potential that yields the highest mole fraction of the MV state is corrected for the absorbance of the neutral species and the 2e⁻ oxidized state at that potential. Data for $Cp^*_2Ti(C_2Fc)_2CuBr$ are shown as a representative example (Figure 9). Insets in Figure 9 show least-square fits to an ideal Nernst equation and the corresponding mole fractions of each species as a function of the applied potential. Reconstructed spectra of the MV states for $^{TMS}Cp_2Ti(C_2Fc)_2CuBr$, and $Cp_2Ti(C_2Fc)_2CuBr$ (Figure 10) show similar features to that of $Cp^*_2Ti(C_2Fc)_2CuBr$. By contrast, the complexes $(Me_2CpC_2Fc)_2TiCl_2$ and $^{TMS}Cp_2Ti(C_2Fc)(C_2Ph)CuBr$ showed no evidence of consecutive oxidation processes (in agreement with the electrochemical data) and gave good fits to a single oxidation process (Figure 10).

All of the complexes with CuX coordinated between the alkynes show strong absorption bands between 561 and 611 nm that are slightly red-shifted and attenuated in molar absorptivity relative to their parent complexes without CuX. In the Cu-free complexes, this absorption has been established as an Fe^{II} to Ti^{IV} MMCT.[14] The spectroelectrochemical data suggests that this assignment is also appropriate in these complexes with coordinated CuX. Chiefly, this band completely vanishes upon 2e⁻ oxidation of the two Fe^{II} centers. Furthermore, this MMCT is still present in the MV state but shifts to lower energy (Table 3), albeit at about half the molar absorptivity. This is consistent with having only a single Fc remaining that can act as a donor in the Fe^{II} to Ti^{IV} MMCT. The oxidized Fc^+ is more electron poor, and in turn, likely withdraws electron density from the Ti^{IV} center allowing it to be more readily reduced. This results in a shift of the Fe^{II} to Ti^{IV} MMCT to comparatively lower energy. A similar red-shift and decrease in molar absorptivity occurs when one of the ethynylferrocene ligands is replaced with a more electron poor ethynyl ligand such as trifluoropropynyl (C_2CF_3) or 4-ethynyl-α,α,α-trifluorotoluene ($C_2C_6H_4CF_3$).[14]

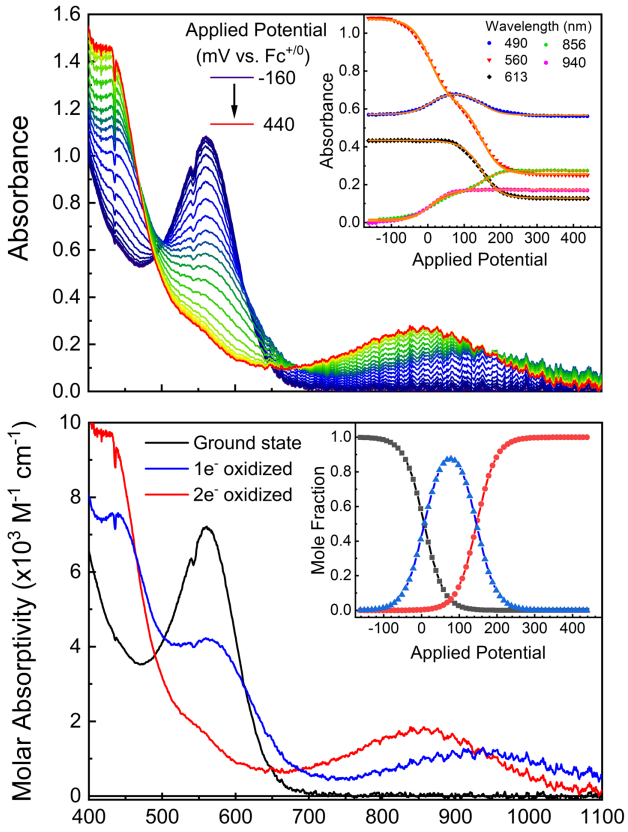

Fig 9: Representative spectroelectrochemical data for $Cp^*_2Ti(C_2Fc)_2CuBr$ (top). Fitted single wavelength data (top inset). Spectra of the ground state, and 2e⁻ oxidized state, and reconstructed spectrum of the 1e⁻ MV state (bottom). Plot of mole fraction of each component vs applied potential (bottom inset). All applied potentials are vs $FcH^{+/0}$.

For the complexes with two separate oxidation processes, both the MV state and the 2e⁻ oxidized state have absorbance features between 793 and 914 nm. The lowest energy absorbance in the MV state gives way to a slightly higher energy absorbance with approximately twice the molar absorptivity in the 2e⁻ oxidized species. These absorbances are assigned to an ethynylcyclopentadienyl to Fe^{III} ligand-to-metal CT (LMCT) based on the following observations: (1) These features occur at higher energy for the Cp* complex than for the Cp or ^{TMS}Cp complexes. This can be rationalized by the more electron rich Cp* ligands providing more electron density on the Ti^{IV} center, and in turn, on the ethynyl ligand. Indeed, the $Ti^{IV/III}$ reduction potential for the Cp* complexes is significantly more cathodic than for the Cp or ^{TMS}Cp complexes.[14,25] (2) The energy of these low-energy absorbances for the MV states of the Cp and ^{TMS}Cp complexes are nearly identical to that of $^{TMS}Cp(C_2Fc)(C_2Ph)CuBr$, where there is only a single Fc (Figure 10, bottom right). This precludes assignment of this spectral feature to an Fe^{II}/Fe^{III} IVCT. (3) When oxidized by 2e⁻, the complex where the C_2Fc donors are covalently bound to the Cp ring on the Ti, i.e. $(Me_2CpC_2Fc)_2TiCl_2$ (Figure 10, top right), shows an absorbance at nearly the same energy as the MV states, albeit with about twice the molar absorptivity. Indeed, this suggests that Cu^I is not involved in the corresponding transitions in the MV states. (4)

Journal Name

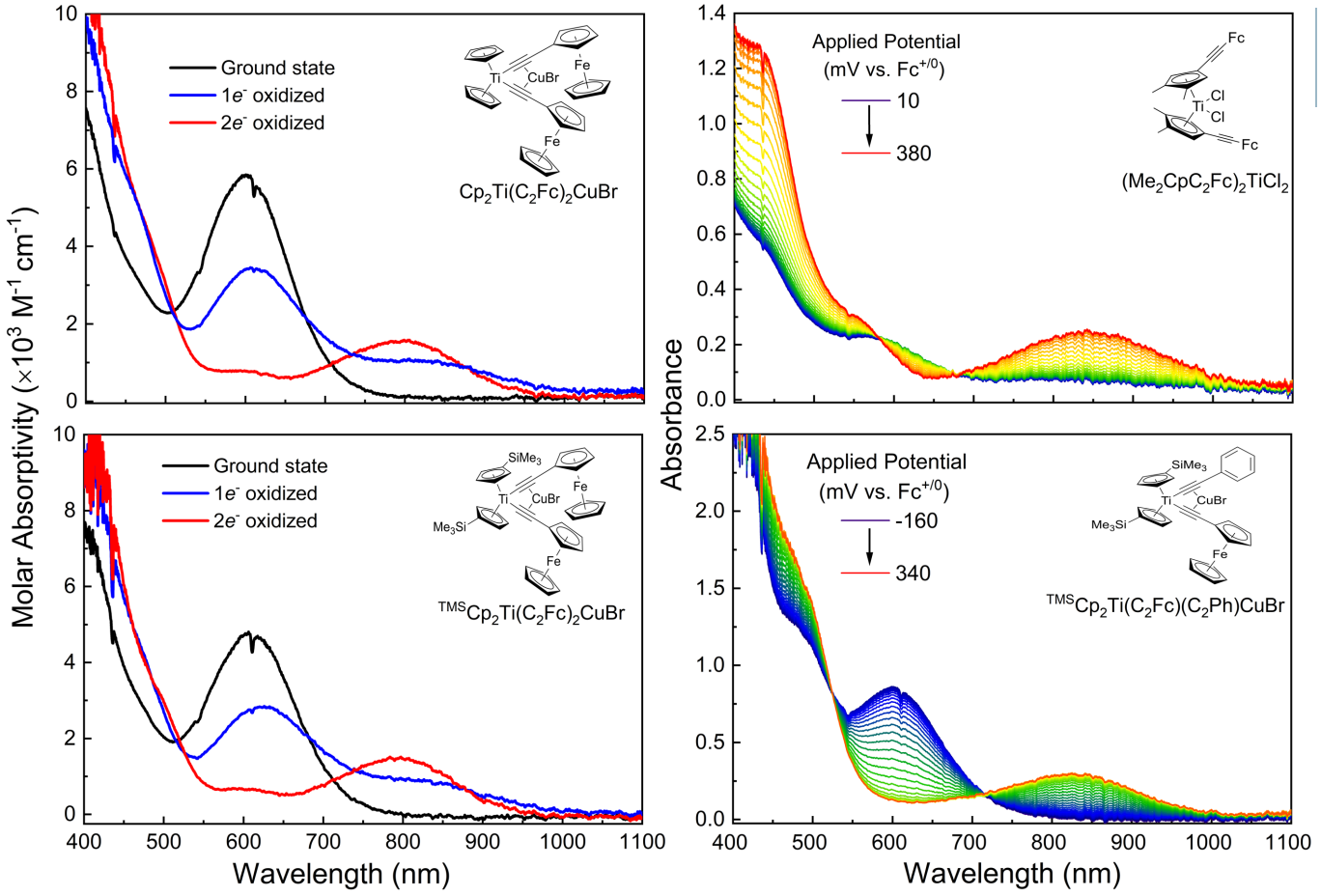

Fig 10: Plots of the neutral ground state, the two electron oxidized state and the reconstructed spectrum of the MV state for $Cp_2Ti(C_2Fc)_2CuBr$ (top left), and $^{TMS}Cp_2Ti(C_2Fc)_2CuBr$ (bottom left) and of the spectroelectrochemical data for $(Me_2CpC_2Fc)_2TiCl_2$ (top right) and $^{TMS}Cp_2Ti(C_2Fc)(C_2Ph)CuBr$ (bottom right).

Spectroelectrochemistry on other systems with ethynylferrocene substituents reveals absorbances between 800 and 1100 nm in the oxidized species that have been assigned as LMCT.[39, 48, 49]

Given the lack of an observable Fe^{II}/Fe^{III} IVCT band in the spectroelectrochemical data (400-1100 nm), redox titrations using $Cu(ClO_4)_2$ were performed and the NIR absorption spectrum was recorded from 850 nm to 2200 nm. Upon the addition of one equivalent of oxidant, the MV state was clearly forming as evidenced by the appearance of the previously described LMCT, yet no lower energy bands were detected (Supporting Information). Given the detection limits of this experiment, we estimate that if an Fe^{II}/Fe^{III} IVCT absorption is present, it must be very weak (< 200 M^{-1} cm^{-1}). This is in agreement with DFT calculations and Mulliken spin density distributions on the singly oxidized $Cp_2Ti(C_2Fc)_2CuBr^+$ (Supporting Information). Such calculations are often used to investigate the degree of charge delocalization in MV states.[50-52] For $Cp_2Ti(C_2Fc)_2CuBr^+$, the spin population is localized on a single Fc.

Interestingly, there appears to be a correlation between the redox splitting, $\Delta E_{1/2}$, and the energy difference between the LMCT in the $2e^-$ oxidized species and the MV state, ΔE_{LMCT} (Table 3). Namely, larger $\Delta E_{1/2}$ values correspond to larger values of ΔE_{LMCT}, with the LMCT of the $2e^-$ oxidized species being higher in energy than that of the MV state. Such an apparent correlation deserves some discussion. If there were no through-bond interactions between the two C_2Fc substituents, and rather only electrostatic interactions between the terminal Fc^+, one would expect the LMCT in the $2e^-$ oxidized species to occur at lower energy than in the MV state. This expectation is due to the through-space electrostatic withdrawing force that one Fc^+ cation would have on the other, therefore anodically shifting the reduction potential of the second Fc^+ (as is observed in the electrochemistry). It follows that the corresponding LMCT would be lower in energy. What is instead observed is the opposite energy ordering which suggests that oxidation of the second Fc has an electron withdrawing effect on the ethynyl ligand of the first, shifting the ethynylcyclopentadienyl to Fe^{III} LMCT transition to higher energy in the $2e^-$ oxidized species vs the MV

Table 3: Spectroscopic properties of the neutral, 1e⁻ oxidized, and 2e⁻ oxidized states.

Compound	neutral MMCT	1e⁻ oxidized MMCT[a]	1e⁻ oxidized LMCT[a]	2e⁻ oxidized LMCT	ΔE_{LMCT}[b] (mV)
$Cp^*_2Ti(C_2Fc)_2CuBr$	561	576	914	857	91
$^{TMS}Cp_2Ti(C_2Fc)_2CuBr$	611	627	816	793	44
$Cp_2Ti(C_2Fc)_2CuBr$	601	610	821	797	45
$Cp_2Ti(C_2Fc)_2CuCl$	601	608	824	797	51
$^{TMS}Cp(C_2Fc)(C_2Ph)CuBr$	600	-	823	-	-
$(Me_2CpC_2Fc)_2TiCl_2$	571	-	-	842	-

[a] Due to closely spaced bands in the MV states, these values were determined from Gaussian fits of the spectra replotted in wavenumbers (Supporting Information). [b] Energy difference between the LMCT in the 2e⁻ oxidized state and the 1e⁻ oxidized (MV) state.

state. Clearly this effect must dominate over the difference in $Fe^{III/II}$ reduction potentials.

Once again, some degree of through-bond communication between the C_2Fc substituents is implicated. The lack of an apparent IVCT absorption suggests such communication might be (1) inductive or (2) stepwise through a non-innocent bridge. An inductive mechanism simply acknowledges that oxidation of one Fc will affect bonding of the ethynyl linker to both the Ti^{IV} and Cu^{I} bridging metals, in turn inducing a shift of the redox potential of the second Fc.[21] As an example of inductive effects, a series of 2,5-diferocenyl substituted furan, thiophene, and N-arylpyroles were investigated in CH_2Cl_2 / [*n*-Bu_4N][$B(C_6F_5)_4$].[45] The contribution to $\Delta E_{1/2}$ from the sum of electrostatic and inductive effects was determined to be 173 mV. Though the bridge in these diferocenyl compounds is quite different than for the titanocenes, contributions of a similar magnitude for the complexes investigated herein cannot be ruled out.

The absence of an experimentally observable IVCT transition alone does not prevent the Fc termini from electronic coupling through a so-called stepwise superexchange mechanism.[22, 47] The appearance of low-energy LMCT transitions following one- and two-electron oxidation suggests possible involvement of the ethynylcyclopentadienyl ligands as non-innocent bridging ligands. This alternative model for communication in the MV state may arise through interactions beyond the traditional 2-state model.[53] Chiefly, the addition of CuX that enables oxidative stability may also allow access to a mediating state involving Cu-centered orbitals. Though the addition of CuX does not give rise to any additional optical transitions that can be assigned as Cu centered, a superexchange interaction would rely on significant mixing between the ethynyl ligands and CuX orbitals as is evident in the HOMO of these compounds. Such a pathway in the MV state might involve hole transfer from Fe^{III} to the ethynylcyclopentadienyl ligand, followed by Cu mediated hole transfer to the opposing ethynylcyclopentadienyl ligand and then to Fe^{II}.[54]

Correlation of $\Delta E_{1/2}$ with Spectroscopic and Electrochemical Parameters

Again, a notable feature is the fact that the electronic communication between the Fc- groups is observed only when Cu^{I} is coordinated in $^{R}Cp_2Ti(C_2Fc)_2$. A comparable value of $\Delta E_{1/2}$ for *cis*-$[Ru(dppm)_2(C_2Fc)_2]CuI$ ($\Delta E_{1/2}$ = 140 mV) was reported,[22] but in that study it was not possible to determine the impact that CuI had on $\Delta E_{1/2}$ because of the instability of *cis*-$[Ru(dppm)_2(C_2Fc)_2]$. Nevertheless, it was hypothesized that Cu^{I} could either act as a second bridge between the two C≡C bonds, enhancing the interactions between Fc- termini, or reducing the conjugation between the metal centers, thereby diminishing the interactions. The fact that Cu^{I} in the titanocene systems is required to observe redox splitting suggests electronic interactions are enhanced by the Cu^{I} bridge. Thus, we hypothesized that the value of $\Delta E_{1/2}$ might correlate with the spectroscopic and/or electrochemical properties of the bridge. Therefore, two series of compounds were compared; $^{R}Cp_2Ti(C_2Fc)_2CuBr$, where the electronics of the Cp ring was varied; and $Cp_2Ti(C_2Fc)_2CuX$ (X = Br, Cl, I), where the halide was modified. First, we hypothesized that $\Delta E_{1/2}$ would be sensitive to the degree of interaction between Cu^{I} and the alkynyl bridge. Because Cu^{I}-alkynyl bonding interactions are revealed in the triple bond stretching frequencies, the alkynyl stretching frequencies ($\upsilon_{C\equiv C}$) of both the $^{R}Cp_2Ti(C_2Fc)_2CuX$ and $Cp_2Ti(C_2Fc)_2$ (Cu-free) titanocenes along with their differences ($\Delta\upsilon_{C\equiv C}$) were compared to the observed $\Delta E_{1/2}$ values (Table 4). There appears to be no clear correlation between the $\upsilon_{C\equiv C}$ values or the $\Delta\upsilon_{C\equiv C}$ value and the $\Delta E_{1/2}$. In the $^{R}Cp_2Ti(C_2Fc)_2CuBr$ series, this is clearly indicated by the fact that $Cp^*_2Ti(C_2Fc)_2CuBr$ has the largest $\Delta E_{1/2}$ but has the second largest $\upsilon_{C\equiv C}$ and $\Delta\upsilon_{C\equiv C}$. In the $Cp_2Ti(C_2Fc)_2CuX$ series, changing the nature of the halide results in insignificant differences in $\upsilon_{C\equiv C}$, $\Delta\upsilon_{C\equiv C}$, and $\Delta E_{1/2}$.

While there is no clear correlation between vibrational frequencies and $\Delta E_{1/2}$ values, the electron density on the $^{R}Cp_2Ti(C_2Fc)_2CuBr$ derivatives, as indicated by the $Ti^{IV/III}$ reduction potentials of the parent $^{R}Cp_2Ti(C_2Fc)_2$ compounds, tracks with the $\Delta E_{1/2}$ values (Table 4). Chiefly, $Cp^*_2Ti(C_2Fc)_2CuBr$, being the most electron rich titanocene, has the largest $\Delta E_{1/2}$ value, whereas the less electron rich titanocenes have $\Delta E_{1/2}$ values that are more closely clustered (117 ± 5 mV). A parallel observation is noted with *trans*-$(Fc\text{-}C\equiv C)_2(PBu_3)_2Ru(CO)(L)$ (Fig. 6, d), where an electron rich ligand (L = C_5H_5N or $P(OMe_3)_3$) produces a larger $\Delta E_{1/2}$ value compared to a π-acid group (L = CO).[22] This result is interpreted in terms of the amount of electron density available on Ru^{II} for conjugation to the acetylide ligands. Likewise, for the 2,5-diferrocenyl–substituted *N*-substituted pyrroles, a correlation was found where the more electron-rich heterocycle bridges resulted in larger $\Delta E_{1/2}$ values.[45]

Table 4: Comparison of $\upsilon_{C\equiv C}$ values, $\Delta\upsilon_{C\equiv C}$, and $E_{1/2}(Ti^{IV/III})$ to $\Delta E_{1/2}$.

Compound	$\upsilon_{C\equiv C}$[a]	$\upsilon_{C\equiv C\ (Cu\text{-}free)}$[a]	$\Delta\upsilon_{C\equiv C}$[a]	$E_{1/2}$ ($Ti^{IV/III}$)[b]	$\Delta E_{1/2}$[c]
$Cp^*_2Ti(C_2Fc)_2CuBr$	2005	2056	51	-2.28	146
$^{TMS}Cp_2Ti(C_2Fc)_2CuBr$	1973	2055	82	-1.76	122
$Cp_2Ti(C_2Fc)_2CuBr$	2006	2053	47	-1.75	112
$Cp_2Ti(C_2Fc)_2CuCl$	2006	2053	47	-1.75	116
$Cp_2Ti(C_2Fc)_2CuI$	2008	2053	45	-1.75	118

[a]Stretching frequencies reported in cm^{-1}. [b]The $E_{1/2}$ ($Ti^{IV/III}$) values (V) of the $^{R}CpTi(C_2Fc)_2$ compounds were used because the $Ti^{IV/III}$ reduction is irreversible in the $^{R}Cp_2Ti(C_2Fc)_2CuX$ species. [c]The $\Delta E_{1/2}$ values (mV) were calculated from the Gaussian fits of the peak-to-peak separation in the DPV.

Experimental Section

General Remarks

THF, Et_2O, and CH_2Cl_2 were dried and degassed using an Innovative Technology Inc. solvent purification system. All other materials were reagent grade and used as received. Reactions were performed under a dry Ar atmosphere implementing standard Schlenk procedures unless otherwise noted. $Cp_2Ti(C_2Ph)_2$,[14] $^{TMS}Cp_2Ti(C_2Fc)(C_2Ph)$,[14] $Cp_2Ti(C_2Fc)_2$,[14] $Cp^*_2Ti(C_2Fc)_2$,[14] $^{TMS}Cp_2Ti(C_2Fc)_2CuBr$,[27] Me_2CpC_2Fc,[18] and $[n\text{-}Bu_4N][B(C_6F_5)_4]$[55] were synthesized according to literature procedures. UV-Visible and NIR absorption spectra were recorded using Cary-50 and Cary-5000 spectrophotometers, respectively. NMR spectra were obtained using a Varian 400-MR or an INOVA 500 spectrometer. Infrared spectra were measured on solid samples using a Perkin-Elmer Spectrum 100 series FT-IR spectrometer equipped with an ATR accessory. Cyclic voltammograms were recorded using a BASi Epsilon electrochemical workstation and a BASi cell stand. Spectroelectrochemistry was performed using a Pt honeycomb electrode with a Pt counter electrode (Pine Research Instruments) and a nonaqueous pseudo Ag/AgCl reference electrode. Spectra were collected using an Avantes AvaLight DHc light source with an Avantes StarLine AvaSpec-2048 UV/Vis spectrometer while the electrochemical potential was applied using a Pine Wavenow potentiostat. All of the devices were controlled by Aftermath software (Pine Research Instruments). For all electrochemical experiments, the $FcH^{+/0}$ potential was measured before and/or after each experiment and all reported potentials are referenced vs this standard. Elemental analyses were performed by Midwest Microlabs in Indianapolis, IN. Gaussian 16 was used for all computational modelling and Gaussview was used for task preparation and orbital imaging.

Syntheses

General method for $^{R}Cp_2Ti(C_2R)_2CuX$
To an oven-dried 50 mL two-neck round bottom flask under a positive pressure of argon was added 0.100 g of the desired titanocene, the appropriate copper halide (2 eq relative to the titanocene), and THF (10 mL). This solution was then allowed to stir for 2h. The following workup was performed without the need of an inert atmosphere. The solvent was removed from the reaction by rotary evaporation. The solid was then loaded onto a silica gel column (0.5 in × 6 in), which was packed and eluted using a 5% solution of triethylamine in CH_2Cl_2. The colored band was collected and the solvent was then removed using rotary evaporation. The resulting solid was dissolved in minimal CH_2Cl_2 (2 mL) and precipitated with hexanes (25 mL). The solid was collected using vacuum filtration, washed with Et_2O (2 mL), and dried under vacuum.

$Cp_2Ti(C_2Fc)_2CuCl$. Using $Cp_2Ti(C_2Fc)_2$ (100 mg, 0.17 mmol) and CuCl (34 mg, 0.34 mmol) resulted in 77 mg (66%) of a dark-green solid. UV/Vis (CH_2Cl_2), λ/nm (ϵ/dm^3 mol^{-1} cm^{-1}): 601 (5278), 361 (9804). UV/Vis (THF), λ/nm (ϵ/dm^3 mol^{-1} cm^{-1}): 597 (3,498), 360 (9610). ^{1}H NMR (400 MHz, $CDCl_3$) δ 6.06 (s, 10H), 4.75 (dd, $J_1 = J_2 = 1.78$ Hz, 4H), 4.31 (dd, $J_1 = J_2 = 1.78$ Hz, 4H), 4.24 (s, 10 H). ^{13}C NMR (400 MHz, $CDCl_3$) δ 142.8, 140.5, 123.1, 110.2, 72.3, 70.3, 69.8, 66.0. Anal. Calcd (found) for $C_{34}H_{28}BrCuFe_2Ti \bullet 2H_2O$: C, 55.85 (55.66); H, 4.41 (4.55). IR (neat) $\nu_{C\equiv C}$ = 2006 cm^{-1}.

$Cp_2Ti(C_2Fc)_2CuBr$. Using $Cp_2Ti(C_2Fc)_2$ (100 mg, 0.17 mmol) and CuBr (49 mg, 0.34 mmol) resulted in 70 mg (56%) of a dark-green solid. UV/Vis (CH_2Cl_2), λ/nm (ϵ/dm^3 mol^{-1} cm^{-1}): 601 (5828), 363 (10,349). UV/Vis (THF), λ/nm (ϵ/dm^3 mol^{-1} cm^{-1}): 590 (3,160), 361 (9,868). ^{1}H NMR (400 MHz, $CDCl_3$) δ 6.07 (s, 10H), 4.72 (dd, $J_1 = J_2 = 1.87$ Hz, 4H), 4.32 (dd, $J_1 = J_2 = 1.88$ Hz, 4H), 4.23 (s, 10H). ^{13}C NMR (400 MHz, $CDCl_3$) δ 143.7, 141.1, 110.2, 72.6, 70.4, 69.9, 66.1. Anal. Calcd (found) for $C_{34}H_{28}BrCuFe_2Ti$: C, 55.22 (55.53); H, 3.82 (4.06). IR (neat) $\nu_{C\equiv C}$ = 2006 cm^{-1}

$Cp_2Ti(C_2Fc)_2CuI$. Using $Cp_2Ti(C_2Fc)_2$ (100 mg, 0.17 mmol) and CuI (48 mg, 0.33 mmol) resulted in 107 mg (81%) of a dark-green solid. UV/Vis (CH_2Cl_2), λ/nm (ϵ/dm^3 mol^{-1} cm^{-1}): 617 (6555), 411 (9792), 368 (11,256). UV/Vis (THF), λ/nm (ϵ/dm^3 mol^{-1} cm^{-1}): 584 (2,937), 361 (11,556). ^{1}H NMR (400 MHz, $CDCl_3$) δ 6.08 (s, 10H), 4.69 (dd, $J_1 = J_2 =$ 1.88 Hz, 4H), 4.34 (dd, $J_1 = J_2 = 1.87$ Hz, 4H), 4.23 (s, 10H). ^{13}C NMR (400 MHz, $CDCl_3$) δ 144.8, 143.5, 141.2,139.5, 132.2, 128.8, 128.3, 123.9, 122.4, 117.4, 117.2, 114.0, 114.0, 73.2, 70.2, 69.5, 67.0, 0.3. IR (neat) $\nu_{C\equiv C}$ = 2008 cm^{-1}.

$Cp^*_2Ti(C_2Fc)_2CuBr$. Using $Cp^*_2Ti(C_2Fc)_2$ (100 mg, 0.14 mmol) and CuBr (39 mg, 0.27 mmol) resulted in 104 mg (87%) of a deep red solid. UV/Vis (CH_2Cl_2), λ/nm (ϵ/dm^3 mol^{-1} cm^{-1}): 561 (7226), 369 (9372). UV/Vis (THF), λ/nm (ϵ/dm^3 mol^{-1} cm^{-1}): 564 (4,842), 369 (9,913). ^{1}H NMR (400 MHz, $CDCl_3$) δ 4.63 (dd, $J_1 = J_2 = 1.89$ Hz, 4H), 4.27 (dd, $J_1 = J_2 = 1.90$ Hz, 4H), 4.22 (s, 10H), 1.99 (s, 30H). ^{13}C NMR (400 MHz, $CDCl_3$) δ 147.4, 134.2, 120.9, 72.0, 70.0, 69.2, 68.0, 13.1. Anal. Calcd (found) for $C_{44}H_{48}BrCuFe_2Ti$: C, 60.06 (60.16); H, 5.50 (5.48). IR (neat) $\nu_{C\equiv C}$ = 2005 cm^{-1}.

$Cp_2Ti(C_2Ph)_2CuBr$. Using $Cp_2Ti(C_2Ph)_2$ (100 mg, 0.26 mmol) and CuBr (76 mg, 0.53 mmol) resulted in 101 mg (73%) of a red solid. UV/Vis (CH_2Cl_2), λ/nm (ϵ/dm^3 mol^{-1} cm^{-1}): 488 (5042), 413 (9966). UV/Vis (THF), λ/nm (ϵ/dm^3 mol^{-1} cm^{-1}): 491 (3,960), 400 (8,944), 377 (8,580). ^{1}H NMR (400 MHz, $CDCl_3$) δ 7.64 (d, J = 6.69 Hz, 4H), 7.44-7.27 (m, 6H), 6.12 (s, 10H). ^{13}C NMR (400 MHz, $CDCl_3$) δ 144.7, 139.0, 132.6, 129.2, 128.3, 123.6, 110.7. Calcd (found) for $C_{26}H_{20}BrCuTi \bullet 0.5\ Et_2O$: C, 59.96 (59.90); H, 4.49 (4.37). IR (neat) $\nu_{C\equiv C}$ = 2001 and 1968 cm^{-1}.

$^{TMS}Cp_2Ti(C_2Fc)(C_2Ph)CuBr$. Using $^{TMS}Cp_2Ti(C_2Fc)(C_2Ph)$ (20.4 mg, 0.032 mmol), CuBr (11.5 mg, 0.080 mmol), and THF (2 mL) resulted in 18.4 mg (74%) of a green solid. Instead of performing the aforementioned reprecipitation, this compound was washed with hexanes (3 x 5 mL) following column chromatography. UV/Vis (CH_2Cl_2), λ/nm (ϵ/dm^3 mol^{-1} cm^{-1}): 600 (3026), 384 (10,013). UV/Vis (CH_2Cl_2), λ/nm (ϵ/dm^3 mol^{-1} cm^{-1}): 491 (3,960), 400 (8,944), 377 (8,580). ^{1}H NMR (400 MHz, $CDCl_3$) 7.66 (m, 2H), 7.38-7.30 (m, 3H), 6.26-6.11 (m, 8H), 4.75 (dd, $J_1 = J_2 =$1.9 Hz, 2H), 4.31 (dd, $J_1 = J_2 =$.9 Hz, 2H), 4.25 (s, 5H), 0.29 (s, 18 H). ^{13}C NMR (400 MHz, $CDCl_3$) δ 144.8, 143.5, 141.2, 139.5, 132.2, 128.8, 128.3, 123.9, 122.4, 117.4, 117.2, 114.0, 114.0, 72.3, 70.2, 69.5. IR (neat) $\nu_{C\equiv C}$ = 1979 cm^{-1}. ESI-MS Found (Calculated) for $C_{36}H_{40}Si_2TiFeCuBr$: m/z 773.9971 (773.9977).

Synthesis of $(Me_2CpC_2Fc)_2TiCl_2$
An argon purged oven dried 3-neck 50 mL round bottom flask was charged with 1-ethynylferrocene-3,4-dimethylcyclopent-1,3-diene (340 mg, 1.13 mmol), and THF (10 mL), and fitted with a 10 mL addition funnel and a gas inlet connected to an argon line. After chilling the solution in a dry ice/acetone bath for 10 min, 2.5 M *n*-BuLi (0.450 mL, 1.13 mmol) was added using a syringe. The mixture

was removed from the dry ice/acetone bath, and stirred at room temperature under argon for 1 h. The addition funnel was loaded with dry THF (10 mL), and 1 M solution of $TiCl_4$ in toluene (0.513 mL, 0.513 mmol), and the resulting solution was added dropwise to the reaction flask over a period of 10 min. The mixture was stirred for 18 h at room temperature under argon. The following workup was performed without the need of an inert atmosphere. After evaporation of the solvents, the resulting brown solid was dissolved in CH_2Cl_2 (30 mL), and filtered through a celite plug. The celite plug was washed with CH_2Cl_2 (30 mL). After evaporation of the solvents from the filtrate, diethyl ether (5 mL) was added to the brown residue. The mixture was sonicated for 30 sec, filtered and the resulting solid was washed with diethyl ether (5×1 mL), yielding 217 mg (59%) of the product isolated as a brown solid. UV/Vis (CH_2Cl_2), λ/nm (ϵ/dm^3 mol^{-1} cm^{-1}): 575 (1,550), 435 (sh, 4,260), 279 (27,000). ^{1}H NMR (500 MHz, $CDCl_3$) δ 6.62 (s, 4H), 4.48 (t, *J* = 1.71 Hz, 4H), 4.29 (t, *J* = 1.71 Hz, 4H), 4.25 (s, 10H), 2.21 (s, 12H). ^{13}C NMR (400 MHz, $CHCl_3$) δ 132.4, 126.3, 107.8, 94.3, 80.2, 71.5, 69.8, 69.1, 64.1, 13.9. Anal. Calcd (found) for $C_{38}H_{34}Cl_2Fe_2Ti$: C, 63.29 (63.65); H, 4.75 (4.87). IR (neat) $\nu_{C\equiv C}$ = 2214 cm^{-1}.

Conclusions

In summary, $(Me_2CpC_2Fc)_2TiCl_2$ and compounds of the form $^RCp_2Ti(C_2Fc)_2CuX$ with Fe^{II} to Ti^{IV} MMCT absorptions were synthesized and their oxidative stability was demonstrated. Indeed Cu^I stabilization allowed the direct spectroscopic and electrochemical observation of the one-electron oxidized MV state and the two-electron oxidized forms. Structural considerations and investigations using supporting electrolytes of varying ion-paring abilities suggests that the observed redox splitting may involve a significant through-bond component. However, despite DFT calculations on $Cp_2Ti(C_2Fc)_2CuBr$ showing that the HOMO is delocalized across both ethynylferrocene ligands and also involves a contribution from the CuBr, no Fe^{II}/Fe^{III} IVCT was observed in the NIR absorption spectrum. There is a relatively low energy (850 nm) absorption in the MV state that gives way to a higher energy (800 nm) transition in the dication. However, this 850 nm feature also exists in an analogous complex with only a single Fc. This absorption has thus been ascribed to an ethynylcyclopentadienyl to Fe^{III} LMCT. This underscores the importance of not only investigating the spectroscopic features of the 2e$^-$ oxidized state, but also of appropriate model compounds with only a single redox site when possible. Though rotation of the Fc substituents in solution makes it impossible to completely rule out through-space electrostatic interactions as contributing to the redox splitting, we have suggested two possible mechanisms for through-bond electronic communication, namely an inductive effect or stepwise coupling through a redox active bridge. This study once again highlights the importance of augmenting electrochemical studies with spectroscopic studies when investigating electronic communication in MV states.[21]

Conflicts of interest

There are no conflicts of interest to declare.

Acknowledgements

This material is based on work supported by the National Science Foundation under the grant CHE-1362516 and in part by an NSF-REU award to the Department of Chemistry at Furman University (CHE-1460806). The University of North Carolina authors gratefully acknowledge support from the Division of Chemical Sciences, Office of Basic Energy Sciences, Office of Energy Research, US Department of Energy (Grant DE-SC0013461). A portion of this work was performed using a Cary 5000 UV/Vis/NIR spectrometer in the UNC EFRC Instrumentation Facility established by the UNC EFRC Center for Solar Fuels, an Energy Frontier Research Center funded by the U.S. Department of Energy, Office of Science, Office of Basic Energy Sciences under Award DE-SC0001011. A.D.A., D.Y.P., and A.B.W. acknowledge support from the Furman Summer Fellows Program. We would like to thank Zachary P. Kolat for helping synthesize precursors.

References

1. T.-D. Kim and K.-S. Lee, *Macromolecular Rapid Communications*, 2015, **36**, 943-958.
2. B. E. Hardin, H. J. Snaith and M. D. McGehee, *Nature Photonics*, 2012, **6**, 162.
3. A. Mishra, M. K. R. Fischer and P. Bäuerle, *Angewandte Chemie International Edition*, 2009, **48**, 2474-2499.
4. C. Schubert, J. T. Margraf, T. Clark and D. M. Guldi, *Chemical Society Reviews*, 2015, **44**, 988-998.
5. H. Imahori, D. M. Guldi, K. Tamaki, Y. Yoshida, C. Luo, Y. Sakata and S. Fukuzumi, *Journal of the American Chemical Society*, 2001, **123**, 6617-6628.
6. S. Kaur, M. Kaur, P. Kaur, K. Clays and K. Singh, *Coordination Chemistry Reviews*, 2017, **343**, 185-219.
7. M. L. H. Green, S. R. Marder, M. E. Thompson, J. A. Bandy, D. Bloor, P. V. Kolinsky and R. J. Jones, *Nature*, 1987, **330**, 360.
8. M. Cariello, S. Ahn, K.-W. Park, S.-K. Chang, J. Hong and G. Cooke, *RSC Advances*, 2016, **6**, 9132-9138.
9. R. Chauhan, R. Yadav, A. K. Singh, M. Trivedi, G. Kociok-Kohn, A. Kumar, S. Gosavi and S. Rane, *RSC Advances*, 2016, **6**, 97664-97675.
10. R. Maragani, R. Misra, M. S. Roy, M. K. Singh and G. D. Sharma, *Physical Chemistry Chemical Physics*, 2017, **19**, 8925-8933.
11. R. Chauhan, M. Trivedi, L. Bahadur and A. Kumar, *Chemistry – An Asian Journal*, 2011, **6**, 1525-1532.
12. R. Chauhan, M. Shahid, M. Trivedi, D. P. Amalnerkar and A. Kumar, *European Journal of Inorganic Chemistry*, 2015, **2015**, 3700-3707.
13. R. Yadav, A. Singh, G. Kociok-Kohn, R. Chauhan, A. Kumar and S. Gosavi, *New Journal of Chemistry*, 2017, **41**, 7312-7321.
14. M. D. Turlington, J. A. Pienkos, E. S. Carlton, K. N. Wroblewski, A. R. Myers, C. O. Trindle, Z. Altun, J. J. Rack and P. S. Wagenknecht, *Inorganic Chemistry*, 2016, **55**, 2200-2211.
15. M. S. Paley and J. M. Harris, *The Journal of Organic Chemistry*, 1991, **56**, 568-574.
16. V. N. Nemykin, E. A. Makarova, J. O. Grosland, R. G. Hadt and A. Y. Koposov, *Inorganic Chemistry*, 2007, **46**, 9591-9601.
17. J. A. Pienkos, A. D. Agakidou, C. O. Trindle, D. W. Herwald, Z. Altun and P. S. Wagenknecht, *Organometallics*, 2016, **35**, 2575-2578.

18. M. Joudat, J. Rouzaud, A. Castel, F. Delpech, P. Rivière, H. Gornitzka and S. Massou, *Inorganica Chimica Acta*, 2004, **357**, 259-264.
19. S. Back, G. Rheinwald and H. Lang, *Journal of Organometallic Chemistry*, 2000, **601**, 93-99.
20. N. D. Jones, M. O. Wolf and D. M. Giaquinta, *Organometallics*, 1997, **16**, 1352-1354.
21. R. F. Winter, *Organometallics*, 2014, **33**, 4517-4536.
22. Y. Zhu, O. Clot, M. O. Wolf and G. P. A. Yap, *Journal of the American Chemical Society*, 1998, **120**, 1812-1821.
23. D. Osella, O. Gambino, C. Nervi, M. Ravera, M. V. Russo and G. Infante, *Inorganica Chimica Acta*, 1994, **225**, 35-40.
24. W. P. Forrest, Z. Cao, H. R. Hambrick, B. M. Prentice, P. E. Fanwick, P. S. Wagenknecht and T. Ren, *European Journal of Inorganic Chemistry*, 2012, **2012**, 5616-5620.
25. S. Back, H. Pritzkow and H. Lang, *Organometallics*, 1998, **17**, 41-44.
26. N. C. Vieira, J. A. Pienkos, C. D. McMillen, A. R. Myers, A. P. Clay and P. S. Wagenknecht, *Dalton Transactions*, 2017, **46**, 15195-15199.
27. S. Back, T. Stein, W. Frosch, I.-Y. Wu, J. Kralik, M. Büchner, G. Huttner, G. Rheinwald and H. Lang, *Inorganica Chimica Acta*, 2001, **325**, 94-102.
28. Y. Hayashi, M. Osawa and Y. Wakatsuki, *Journal of Organometallic Chemistry*, 1997, **542**, 241-246.
29. N. Elgrishi, K. J. Rountree, B. D. McCarthy, E. S. Rountree, T. T. Eisenhart and J. L. Dempsey, *Journal of Chemical Education*, 2018, **95**, 197-206.
30. Greef, R.; Peat, R.; Peter, L. M.; Pletcher, D.; Robinson, J. Instrumental Methods in Electrochemistry; Ellis Horwood: Chichester, U.K., 1985.
31. D. E. Richardson and H. Taube, *Inorganic Chemistry*, 1981, **20**, 1278-1285.
32. T. Cheng, M. Meng, H. Lei and C. Y. Liu, *Inorganic Chemistry*, 2014, **53**, 9213-9221.
33. Z. Cao, P. E. Fanwick, W. P. Forrest, Y. Gao and T. Ren, *Organometallics*, 2013, **32**, 4684-4689.
34. T. D. Cook, P. E. Fanwick and T. Ren, *Organometallics*, 2014, **33**, 4621-4624.
35. S. N. Natoli, T. J. Azbell, P. E. Fanwick, M. Zeller and T. Ren, *Organometallics*, 2016, **35**, 3594-3603.
36. S. N. Natoli, M. Zeller and T. Ren, *Inorganic Chemistry*, 2016, **55**, 5756-5758.
37. T. D. Cook, S. N. Natoli, P. E. Fanwick and T. Ren, *Organometallics*, 2016, **35**, 1329-1338.
38. Z. Cao, W. P. Forrest, Y. Gao, P. E. Fanwick and T. Ren, *Organometallics*, 2012, **31**, 6199-6206.
39. U. Pfaff, A. Hildebrandt, M. Korb and H. Lang, *Polyhedron*, 2015, **86**, 2-9.
40. A. Nafady, T. T. Chin and W. E. Geiger, *Organometallics*, 2006, **25**, 1654-1663.
41. F. Barrière, N. Camire, W. E. Geiger, U. T. Mueller-Westerhoff and R. Sanders, *Journal of the American Chemical Society*, 2002, **124**, 7262-7263.
42. A. K. Diallo, C. Absalon, J. Ruiz and D. Astruc, *Journal of the American Chemical Society*, 2011, **133**, 629-641.
43. K.-W. Poon, W. Liu, P.-K. Chan, Q. Yang, T. W. D. Chan, T. C. W. Mak and D. K. P. Ng, *The Journal of Organic Chemistry*, 2001, **66**, 1553-1559.
44. I. Masahiko, K. Terumasa, O. Toshitaka, M. Haruo, S. Shigeru and K. Yoshiyuki, *Chemistry Letters*, 1997, **26**, 35-36.
45. A. Hildebrandt and H. Lang, *Organometallics*, 2013, **32**, 5640-5653.
46. J. M. Speck, R. Claus, A. Hildebrandt, T. Rüffer, E. Erasmus, L. van As, J. C. Swarts and H. Lang, *Organometallics*, 2012, **31**, 6373-6380.
47. E. J. Piechota, L. Troian-Gautier, R. N. Sampaio, M. K. Brennaman, K. Hu, C. P. Berlinguette and G. J. Meyer, *Journal of the American Chemical Society*, 2018, **140**, 7176-7186.
48. F. Strehler, M. Korb, E. A. Poppitz and H. Lang, *Journal of Organometallic Chemistry*, 2015, **786**, 1-9.
49. L. Cuffe, R. D. A. Hudson, J. F. Gallagher, S. Jennings, C. J. McAdam, R. B. T. Connelly, A. R. Manning, B. H. Robinson and J. Simpson, *Organometallics*, 2005, **24**, 2051-2060.
50. M. Parthey and M. Kaupp, *Chemical Society Reviews*, 2014, **43**, 5067-5088.
51. W. Si-Hai, S. Jun-Jian, Y. Jiannian and Z. Yu-Wu, *Chemistry – An Asian Journal*, 2013, **8**, 138-147.
52. G. Zhong-Liang, Z. Yu-Wu and Y. Jiannian, *Chemistry – A European Journal*, 2015, **21**, 1554-1566.
53. C. Creutz, M. D. Newton and N. Sutin, *Journal of Photochemistry and Photobiology A: Chemistry*, 1994, **82**, 47-59.
54. M. Natali, S. Campagna and F. Scandola, *Chemical Society Reviews*, 2014, **43**, 4005-4018.
55. R. J. LeSuer, C. Buttolph and W. E. Geiger, *Analytical Chemistry*, 2004, **76**, 6395-6401.

Table of Contents Entry

Coordination of Cu^{I} into $^{R}Cp_2Ti(C_2Fc)_2$ compounds results in well-separated $Fe^{III/II}$ couples and mixed-valent states with distinct spectroscopic signatures.